Q. J. R. Meteorol. Soc. (2002), **128**, pp. 1159–1171

Maslov's method for stationary hydrostatic mountain waves

By DAVE BROUTMAN[1], JAMES W. ROTTMAN[2] and STEPHEN D. ECKERMANN[3]*

[1]*Computational Physics, Inc., USA*
[2]*Science Applications International Corporation, USA*
[3]*Naval Research Laboratory, USA*

(Received 18 April 2001; revised 12 September 2001)

SUMMARY

The ray solution for stationary hydrostatic mountain waves has a singularity along the vertical axis directly over the mountain. We use Maslov's method to improve the ray prediction. The ray solution is determined in the wave-number domain and is then mapped by inverse Fourier transform to give a spatial description of the wave field that approximates the linear solution over the mountain and elsewhere. We develop Maslov's method for a medium with a height-dependent mean wind and mean buoyancy, and we compare it with the traditional transform method and with the results of a numerical simulation.

KEYWORDS: Caustics Gravity waves Ray tracing

1. INTRODUCTION

In a previous study, we developed a ray-tracing scheme for mountain waves that includes the prediction of wave amplitudes along the ray (Broutman *et al.* 2001). We initialized the rays with a near-field stationary-phase approximation, and we used the ray-tracing to examine the far-field approach to critical layers in three dimensions with rotation. We were unable, however, to analyse the region directly over the mountain. Ray theory is inaccurate there because of the breakdown of the slowly varying approximation.

In the present study we first show that this breakdown is associated with a special type of caustic that cannot be treated by the usual correction techniques, such as an Airy-function matching. We then use Maslov's method to improve the ray prediction. The method was developed in the 1960's by V. P. Maslov as a short-wavelength asymptotic technique for problems in quantum mechanics. An introduction to the method has been given by Maslov and Fedoriuk (1981), Kravtsov and Orlov (1993), Thomson and Chapman (1985), and Ziolkowski and Deschamps (1984). Another helpful reference, on which our own work is most closely based, is Brown (2000).

To derive Maslov's solution, we express the ray solution as a function of wave-number coordinates, rather than in the usual way as a function of spatial coordinates. In wave-number coordinates, the rays in our model remain well separated and do not form caustics. The ray solution is then mapped from the wave-number coordinates to the spatial coordinates by an inverse Fourier transform. The result reproduces the usual spatial ray solution where that ray solution is accurate, but also corrects the caustic singularity in the region over the mountain.

There is another way to derive Maslov's solution, by a variation of the standard transform technique. The difficulty with the standard technique is that the normal modes are required, and these can rarely be expressed in a useful analytical form. Maslov's method amounts to a simplification in which the normal modes are approximated by ray theory. Shutts (1998) has made this simplification in an analysis of hydrostatic mountain waves in a turning wind. We show in section 3(c) that Maslov's method gives Shutts's solution as a special case. The consideration of normal modes also leads to a criterion

* Corresponding author: E. O. Hulburt Center for Space Research, Code 7641, Naval Research Laboratory, 4555 Overlook Ave, SW, Washington, DC 20375-5320, USA. e-mail: eckerman@uap2.nrl.navy.mil

Report Documentation Page

Form Approved
OMB No. 0704-0188

1. REPORT DATE	2. REPORT TYPE	3. DATES COVERED
12 SEP 2001		**00-00-2001 to 00-00-2001**

4. TITLE AND SUBTITLE	5a. CONTRACT NUMBER
Maslov's method for stationary hydrostatic mountain waves	5b. GRANT NUMBER
	5c. PROGRAM ELEMENT NUMBER
6. AUTHOR(S)	5d. PROJECT NUMBER
	5e. TASK NUMBER
	5f. WORK UNIT NUMBER
7. PERFORMING ORGANIZATION NAME(S) AND ADDRESS(ES) **Naval Research Laboratory,E.O. Hulburt Center for Space Research,Washington,DC,20375**	8. PERFORMING ORGANIZATION REPORT NUMBER
9. SPONSORING/MONITORING AGENCY NAME(S) AND ADDRESS(ES)	10. SPONSOR/MONITOR'S ACRONYM(S)
	11. SPONSOR/MONITOR'S REPORT NUMBER(S)

12. DISTRIBUTION/AVAILABILITY STATEMENT
Approved for public release; distribution unlimited

13. SUPPLEMENTARY NOTES

14. ABSTRACT

15. SUBJECT TERMS

16. SECURITY CLASSIFICATION OF:			17. LIMITATION OF ABSTRACT	18. NUMBER OF PAGES	19a. NAME OF RESPONSIBLE PERSON
a. REPORT **unclassified**	b. ABSTRACT **unclassified**	c. THIS PAGE **unclassified**	**Same as Report (SAR)**	**13**	

for the validity of Maslov's solution, which depends on the largeness of the Richardson number. Note that the standard ray method fails over the mountain for all Richardson numbers.

In section 4, we compare Maslov's method with a numerical simulation in Shutts and Gadian (1999), finding reasonable agreement. They study mountain waves in a turning wind using a nonlinear non-hydrostatic model, though their choice of a small wide hill for this simulation favours a linear hydrostatic response.

Throughout this paper we assume linear stationary hydrostatic waves without rotation. The medium is horizontally homogeneous, with smooth height-dependent mean wind and mean buoyancy. These assumptions simplify the implementation of Maslov's method in significant ways. For example, the combination of horizontal homogeneity and hydrostatic waves prevents caustics from occurring in the wave-number coordinates. Maslov's method handles cases in which there are caustics in both spatial and wave-number coordinates, but the implementation is more difficult (e.g. Brown 2000). Other potential difficulties associated with the inclusion of rotation and non-hydrostatic effects are noted at the end of section 3.

We use the Boussinesq approximation until section 4. In that section, Maslov's solution is scaled in the standard way to account for the decrease in mean density with height (Gill 1982, section 6.14). This is necessary for the comparison with the simulation by Shutts and Gadian (1999), whose model uses the anelastic form of the continuity equation.

2. Ray theory for stationary hydrostatic mountain waves

We first describe the traditional ray solution for three-dimensional stationary hydrostatic mountain waves. Examples are given by Smith (1980) for the case of a uniform medium, and by Shutts (1998) and Broad (1999) for cases with wind shear. Our aim here is to understand why ray theory fails directly over the mountain. We use coordinates $\mathbf{x} = (x, y)$ in the horizontal directions and z in the vertical direction. The mean wind is horizontal and has the form $\mathbf{U} = (U(z), V(z))$, and the mean buoyancy frequency is $N(z)$.

The mountain waves have vertical wave number m and horizontal wave-number vector

$$\mathbf{k} = (k, l) = K(\cos\phi, \sin\phi), \tag{1}$$

with magnitude K and angle ϕ from the positive x-axis. We take the positive x-axis to point in the downwind direction at ground level. Then the combination $k < 0$, $m < 0$ and intrinsic frequency $\widehat{\omega} > 0$ gives stationary waves with upward group propagation. The intrinsic frequency and wave number satisfy

$$\widehat{\omega} = -KN/m = -kU - lV. \tag{2}$$

The first relation in (2) is the hydrostatic form of the internal-wave dispersion relation under present assumptions, while the second relation is the condition for stationary waves which, by definition, have zero frequency relative to the ground. The group velocity relative to the ground has horizontal components

$$\mathbf{c}_{\mathrm{g}} = (c_{\mathrm{g}1}, c_{\mathrm{g}2}) = (U - kN/Km, V - lN/Km) \tag{3}$$

and vertical component $c_{\mathrm{g}3} = KN/m^2$.

It is convenient to use z as the independent ray variable, following Shutts (1998) and Broad (1999). The ray path $\mathbf{x}(z)$ is then determined from

$$\mathrm{d}\mathbf{x}/\mathrm{d}z = \mathbf{c}_{\mathrm{g}}/c_{\mathrm{g}3}. \tag{4}$$

All rays are launched from the origin, consistent with a stationary-phase analysis (Broutman *et al.* 2001). Since the medium is horizontally homogeneous, k and l are constant along the ray.

It follows from (3) and (2) that

$$\mathbf{k} \cdot \mathbf{c}_g = 0. \tag{5}$$

It follows from (4), with the initial ray position at the origin, from (5), and from the constancy of $\mathbf{k}$ along the ray, that

$$\mathbf{k} \cdot \mathbf{x} = 0. \tag{6}$$

Therefore

$$\mathbf{x} \parallel \mathbf{c}_g. \tag{7}$$

This shows that the horizontal group velocity vector always lies on a line extending radially from the origin. Each ray is thus constrained to remain in a single vertical plane throughout its propagation. The propagation plane, with equation $x/y = -l/k = -\tan\phi$, passes through the origin and is normal to $(k, l, 0)$. All rays with the same value of ϕ share the same propagation plane. Similar points have been made by Shutts (1998) and by Broad (1999). Note that the conditions (5)–(7) hold only in the hydrostatic limit without rotation.

We illustrate this behaviour with an example taken from the model of Shutts (1998). He considers the wind profile

$$\mathbf{U}(z) = (U_0, \Lambda z), \tag{8}$$

where U_0 and Λ are constants and $z = 0$ is the ground. Shutts's model reduces to that of Smith (1980) when $\Lambda = 0$. In the example plotted below, we set $\Lambda = 0.003\ \mathrm{s}^{-1}$, $U_0 = 10\ \mathrm{m\ s}^{-1}$, and $N = 0.01\ \mathrm{s}^{-1}$, values used in Shutts's calculations.

Two sets of five ray paths each are shown in Figs. 1(a) and (b). The mean-wind profile (8) used in these calculations is indicated in Fig. 1(a). Also indicated by the dashed line in each plot is the projection of the ray paths onto the $z = 0$ plane. The projection is a single straight line because the rays in each set have the same value of ϕ and, therefore, share the same propagation plane. In terms of the polar coordinate angle $\theta = \tan^{-1}(y/x)$, the propagation planes in Figs. 1(a) and (b) are defined by $\theta = 50^\circ$ and $\theta = -50^\circ$ respectively. In our wave-number notation (1) this corresponds to wave-number angles $\phi = 140^\circ$ and $\phi = -140^\circ$, respectively. The five rays in each plot have K values equally spaced between $0.2/L$ and $1/L$, where $L = 20$ km is the mountain width used by Shutts (1998).

Rays that propagate over the first quadrant (Fig. 1(a)) are refracted toward decreasing intrinsic frequency. Each ray asymptotes toward its own critical-layer height. This case was treated in detail by Shutts (1998) without rotation and by Broutman *et al.* (2001) with rotation. These rays never intersect each other after leaving the origin.

Rays that initially propagate over the fourth quadrant (Fig. 1(b)) are refracted toward increasing intrinsic frequency. Their vertical group velocity also increases with height, and they encounter an increasingly strong cross-wind $V(z)$. Eventually, these rays reverse their horizontal direction of propagation, moving upwind in x and downwind in y. The rays loop back over the origin and intersect at a single point on the vertical axis. Rays constrained to other planes with $-\pi/2 < \theta < 0$ focus at other heights on the vertical axis, forming a line of ray singularities. This is why Shutts's stationary-phase solution diverges over the mountain (see Eq. (67) of Shutts 1998).

We can prove the general result illustrated in Fig. 1(b), that all rays in the same propagation plane intersect the vertical axis at the same point. We return to the case of

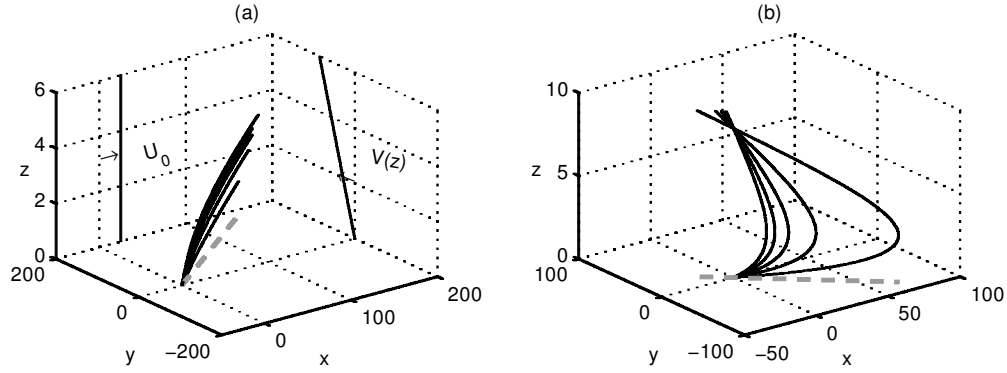

Figure 1. Ray paths for the model of Shutts (1998). The axes are labelled in km, with the mean wind profile indicated in panel (a) only. Rays are terminated after 80 buoyancy periods of propagation. The projection of the ray paths onto the x–y plane is represented by the dashed line. Two types of behaviour are illustrated, depending on whether the rays refract toward lower intrinsic frequency or toward higher intrinsic frequency. In the former case, panel (a), each ray approaches its own critical level. The propagation plane is $\theta = \tan^{-1}(y/x) = 50^\circ$. In the latter case, panel (b), the rays loop over the mountain and intersect at one point on the z-axis. The propagation plane is $\theta = -50^\circ$.

arbitrary $U(z)$, $V(z)$ and $N(z)$. It is sufficient here to work only with the x-coordinate of the ray. When the x-coordinate vanishes, so does the y-coordinate, and the ray has intersected the vertical axis. The ray equation (4) for $x(z)$ becomes

$$x = \int \frac{c_{g1}}{c_{g3}}\,\mathrm{d}z = \frac{\tan\phi}{K}\int N(z)\frac{U(z)\tan\phi - V(z)}{(U(z)+V(z)\tan\phi)^2}\,\mathrm{d}z. \tag{9}$$

The integral in (9) is taken along the ray, and the ray is launched from the origin. The ray position x depends in general on K but, on the vertical axis, $x = 0$ and we are left with a relation for $z(\phi)$ in which the K factor cancels out. Thus all rays in the same propagation plane (determined by ϕ) intersect each other on the vertical axis at precisely the same point (or set of points).

The curve or surface on which neighbouring rays intersect each other is called a caustic (Lighthill 1978; Kravtsov and Orlov 1993; Sonmor and Klaassen 2000). Each neighbouring ray has a slightly different wave number, so the wave-number gradient diverges on the caustic in violation of the slowly varying approximation. The ray prediction for the wave-action density also diverges, depending inversely on the size of a volume element enclosed by the neighbouring rays.

There are standard ways to correct the ray solution near certain types of caustics, but this caustic is not one of those types. The simplest and most familiar caustic is corrected with an Airy function (Lighthill 1978) and is characterized by the intersection of two neighbouring rays at each point on the caustic. More complicated caustics require different correction functions and involve the intersection of more rays. Three neighbouring rays intersect at the tip of a cusped caustic, for example, whose correction function can be found in the monograph by Kravtsov and Orlov (1993).

As we have just shown, the caustic over the mountain is intersected by an infinite number of rays at each point. Such caustics arise only in very special circumstances and are structurally unstable (Berry 1981, p. 480). That is, they generally break apart with a small perturbation to the problem. A minor non-hydrostatic correction, for instance, is

enough to eliminate the mountain-wave caustic entirely. By contrast, the simple Airy-function caustic is one of several kinds of caustics (including the cusped caustic) that survive perturbation and are structurally stable. A slight perturbation to a problem with a stable caustic merely leads, in general, to a slight movement in the caustic's position.

Broutman *et al.* (2001) computed non-hydrostatic ray solutions for the Shutts (1998) model. Although the non-hydrostatic ray paths do not quite intersect over the mountain, they still focus strongly there, causing a breakdown of the slowly varying assumption and erroneously large ray predictions for the vertical displacement. Another way is needed to correct the ray solution, and for this purpose we now turn to Maslov's method.

3. Maslov's method

Maslov's solution is the inverse Fourier transform of the ray solution expressed in wave-number coordinates. To derive Maslov's solution, we start with the more familiar ray solution in spatial coordinates, map it to wave-number coordinates using the local ray relation between wave number and position, apply boundary conditions, and then map back to the spatial coordinates by inverse Fourier transform.

For stationary mountain waves there is no time dependence, and the z-dependence can be treated parametrically. A ray variable describing the waves, such as the vertical displacement, is written in spatial coordinates as

$$\eta(\mathbf{x}, z) = a(\mathbf{x}, z)\, \mathrm{e}^{\mathrm{i}\psi(\mathbf{x},z)} \tag{10}$$

and in wave-number coordinates as

$$\widetilde{\eta}(\mathbf{k}, z) = \widetilde{a}(\mathbf{k}, z)\, \mathrm{e}^{\mathrm{i}\widetilde{\psi}(\mathbf{k},z)}. \tag{11}$$

As before $\mathbf{x} = (x, y)$ and $\mathbf{k} = (k, l)$. The inverse Fourier transform of $\widetilde{\eta}(\mathbf{k}, z)$ gives Maslov's solution

$$\eta_{\mathrm{m}}(\mathbf{x}, z) = \int_{-\infty}^{\infty}\int_{-\infty}^{\infty} \widetilde{\eta}(\mathbf{k}, z)\, \mathrm{e}^{\mathbf{i}\mathbf{k}\cdot\mathbf{x}}\, \mathrm{d}k\, \mathrm{d}l. \tag{12}$$

(*a*) *The spatial domain*

The vertical-displacement amplitude $|a(\mathbf{x}, z)|$ in (10) can be obtained in ray theory from conservation of wave-action. The wave-action density $A(\mathbf{x}, z)$ and the wave-energy density $E(\mathbf{x}, z)$ are related by $A = E/\widehat{\omega}$, where $\widehat{\omega}$ is the intrinsic frequency. For gravity waves without rotation

$$A = \tfrac{1}{2}\rho_0 |a|^2 N^2/\widehat{\omega}, \tag{13}$$

where ρ_0 is the mean density. In a steady-state application such as ours, A satisfies

$$\nabla \cdot (\mathbf{c}_g A) + \partial(c_{\mathrm{g}3} A)/\partial z = 0, \tag{14}$$

where $\nabla = (\partial/\partial x, \partial/\partial y)$. Integration of (14) over a ray-tube volume, followed by an application of the divergence theorem leads to (cf. Broad 1999)

$$c_{\mathrm{g}3}\ A\ \mathrm{J}\left(\frac{x,\ y}{x_0,\ y_0}\right) = \text{constant} \tag{15}$$

following the ray. Here $x_0,\ y_0$ is an initial point on the ray corresponding to $z = z_0$.

The Jacobian in (15), defined by

$$\mathrm{J}\left(\frac{x,\ y}{x_0,\ y_0}\right) = \frac{\partial x}{\partial x_0}\frac{\partial y}{\partial y_0} - \frac{\partial x}{\partial y_0}\frac{\partial y}{\partial x_0}, \tag{16}$$

is evaluated at constant z and accounts for the change in A due to the horizontal spreading of rays. The factor of c_{g3} in (15) accounts for the change in A due to the vertical spreading of rays.

The phase ψ in the spatial solution (10) is given by

$$\psi(\mathbf{x}, z) = \mathbf{k}(\mathbf{x}, z) \cdot \mathbf{x} + \int_0^z m(\mathbf{x}, z')\, \mathrm{d}z'. \tag{17}$$

All rays originate from the origin, where $\psi = 0$, consistent with the stationary-phase solution (Shutts 1998; Broutman *et al.* 2001). For the hydrostatic case, we noted in section 2 that $\mathbf{k} \cdot \mathbf{x}$ vanishes. We retain this term for now. It will cancel out below (in (24)) without recourse to the hydrostatic approximation.

(*b*) *The wave-number domain*

Next we determine the wave-number solution $\widetilde{\eta}(\mathbf{k}, z)$ in (11). Starting with conservation of wave-action (15), we re-express the Jacobian using the chain rule to yield

$$c_{g3}\, A\, \mathrm{J}\left(\frac{x, y}{k, l}\right) \mathrm{J}\left(\frac{k, l}{x_0, y_0}\right) = \text{constant}. \tag{18}$$

The product of A with the first Jacobian in (18) transforms the wave-action from a spatial density to a wave-number density $\widetilde{A}(\mathbf{k}, z)$, i.e.,

$$\widetilde{A}(\mathbf{k}, z) = A(\mathbf{x}, z)\, \mathrm{J}\left(\frac{x, y}{k, l}\right). \tag{19}$$

The second Jacobian in (18) is constant along the ray in our problem. Thus

$$c_{g3} \widetilde{A} = \text{constant}. \tag{20}$$

In the wave-number domain, the vertical flux of wave-action is constant following the ray. Figure 2 helps to illustrate this point. The left panel shows rays in the spatial domain. They diverge strongly in all three dimensions as they move away from the mountain centred at the origin. The right panel shows the corresponding rays in the wave-number domain. Being parallel to the z-direction, they diverge or converge only with respect to the z-direction. This implies the form of wave-action conservation given in (20).

Ray initialization is simple in the wave-number domain. The rays can be initialized directly from the mountain profile rather than through the near-field stationary-phase analysis used by Broutman *et al.* (2001) to initialize rays in the spatial domain. The vertical displacement $\widetilde{\eta}(\mathbf{k}, z)$ in (11) is equated at $z = 0$ to the Fourier transform $\widetilde{h}(\mathbf{k})$ of the mountain profile $h(\mathbf{x})$. Since $\widetilde{\psi}$ vanishes at $z = 0$ (see (25) below), we are left with

$$\widetilde{a}(\mathbf{k}, 0) = \widetilde{h}(\mathbf{k}). \tag{21}$$

Next we relate $\widetilde{A}$ to $\widetilde{\eta}$ in (11) by

$$\widetilde{A} = \tfrac{1}{2} \rho_0 |\widetilde{a}|^2 N^2 / \widehat{\omega}, \tag{22}$$

analogous to the definition in the spatial domain (13) and analogous to the plane-wave polarization relations between Fourier amplitudes of different variables (Gill 1982, section 6.5). Combining (20), (21), and (22) yields

$$\widetilde{a}(\mathbf{k}, z) = \widetilde{h}(\mathbf{k}) \left[\frac{c_{g3}(\mathbf{k}, 0)}{c_{g3}(\mathbf{k}, z)} \frac{\widehat{\omega}(\mathbf{k}, z)}{\widehat{\omega}(\mathbf{k}, 0)}\right]^{1/2} \frac{N(0)}{N(z)}. \tag{23}$$

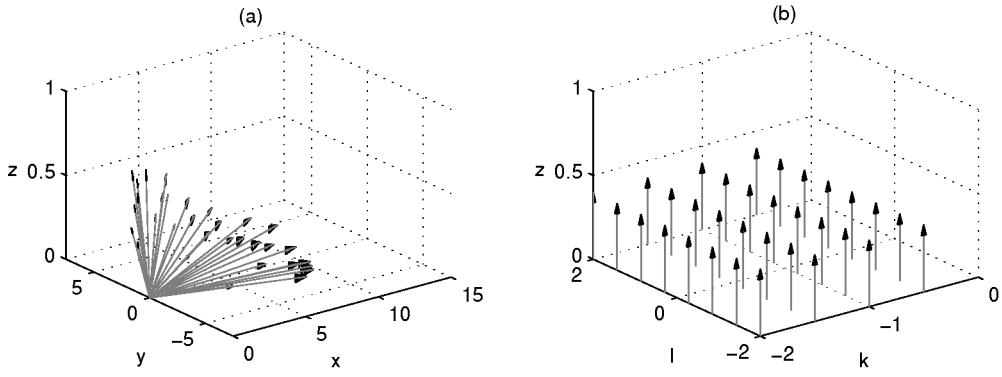

Figure 2. Rays near the mountain in (a) the spatial domain and (b) the wave-number domain. The length of the ray vectors is not significant. The mountain is centred at the origin in (a). The spatial coordinates are labelled in km. The wave-number coordinates k, l are normalized by the mountain width $L = 20$ km. We have ignored refraction because the dominant effect near the mountain is geometrical spreading. Refraction by vertical shear causes the rays to curve in the spatial domain but not in the wave-number domain.

The phase in the wave-number domain $\widetilde{\psi}$ is related to the phase in the spatial-domain ψ by the Legendre transformation (e.g. Brown 2000; Ziolkowski and Deschamps 1984)

$$\widetilde{\psi}(\mathbf{k}, z) = \psi(\mathbf{x}, z) - \mathbf{k} \cdot \mathbf{x}(\mathbf{k}, z). \tag{24}$$

Substituting from (17) gives a cancellation of $\mathbf{k} \cdot \mathbf{x}$ terms, leaving

$$\widetilde{\psi}(\mathbf{k}, z) = \int_0^z m(\mathbf{k}, z')\, \mathrm{d}z'. \tag{25}$$

The cancellation of the $\mathbf{k} \cdot \mathbf{x}$ terms occurs only because $\mathbf{k}$ is constant along the ray. More generally ψ depends on $\int \mathbf{k} \cdot \mathrm{d}\mathbf{x}$, whereas the term in the Legendre transformation is always $\mathbf{k} \cdot \mathbf{x}$.

(c) *The Maslov solution*

Substituting the amplitude solution (23) and the phase solution (25) into the Fourier integral (12) gives the Maslov solution

$$\eta_{\mathrm{m}}(\mathbf{x}, z) = \frac{N(0)}{N(z)} \int_{-\infty}^{\infty} \int_{-\infty}^{\infty} \widetilde{h}(\mathbf{k}) \left[\frac{c_{\mathrm{g}3}(\mathbf{k}, 0)}{c_{\mathrm{g}3}(\mathbf{k}, z)} \frac{\widehat{\omega}(\mathbf{k}, z)}{\widehat{\omega}(\mathbf{k}, 0)} \right]^{1/2} \mathrm{e}^{\mathrm{i} \int_0^z m(\mathbf{k}, z')\, \mathrm{d}z'} \mathrm{e}^{\mathrm{i}\mathbf{k}\cdot\mathbf{x}}\, \mathrm{d}k\, \mathrm{d}l. \tag{26}$$

In the case of a uniform medium, the ratio in square brackets is unity, as is the ratio of N values, and $\int_0^z m(\mathbf{k}, z')\, \mathrm{d}z' = m(\mathbf{k})z$. Thus (26) reduces to the integral solution in the uniform-medium model of Smith (1980, Eq. (11)). For constant N and hydrostatic waves, (26) simplifies to

$$\eta_{\mathrm{m}}(\mathbf{x}, z) = \int_{-\infty}^{\infty} \int_{-\infty}^{\infty} \widetilde{h}(\mathbf{k}) \left[\frac{m(\mathbf{k}, z)}{m(\mathbf{k}, 0)} \right]^{1/2} \mathrm{e}^{\mathrm{i} \int_0^z m(\mathbf{k}, z')\, \mathrm{d}z'} \mathrm{e}^{\mathrm{i}\mathbf{k}\cdot\mathbf{x}}\, \mathrm{d}k\, \mathrm{d}l. \tag{27}$$

We now show that (27) agrees with the solution derived by Shutts (1998) for a particular mean-wind profile. This serves as a check on our derivation and illustrates the relation between Maslov's method and a standard transform method involving normal modes. It also leads to a condition for assessing the validity of Maslov's solution.

Shutts (1998) examines stationary hydrostatic mountain waves in a medium with constant buoyancy frequency N and with mean wind velocity $(U_0, \Lambda z)$, where U_0 and Λ are positive constants and $z = 0$ is the ground. Shutts derives an equation for the normal modes in terms of the coordinate ζ defined by

$$\zeta = \frac{1}{1 + (\Lambda z \tan \phi)/U_0}, \tag{28}$$

where $\phi = \tan^{-1} l/k$. (Shutts's results are given here in his notation, which differs from ours in that his k and m are positive.) The normal-mode equation is

$$\frac{\partial^2 \widetilde{\eta}}{\partial \zeta^2} + \frac{\mu^2}{\zeta^2}\widetilde{\eta} = 0, \tag{29}$$

where $\mu = N/(\Lambda \sin \phi)$. As noted by Shutts, the exact solution to (29) has the form ζ^{ν} with $\nu = 1/2 \pm \mathrm{i}(\mu^2 - 1/4)^{1/2}$.

At this point in his derivation, Shutts makes two assumptions that amount to invoking the ray approximation. First, he assumes that the Richardson number N^2/Λ^2 is large, so that $\mu^2 \gg 1/4$. Secondly, he considers only waves with upward group velocity, corresponding to the negative root in the above expression for ν. This ignores partial reflection, which is also ignored in standard ray theory. After applying the boundary condition at $z = 0$, Shutts finds that

$$\widetilde{\eta} = \zeta^{1/2}\widetilde{h}(\mathbf{k})\, \mathrm{e}^{-\mathrm{i}\mu \log \zeta}. \tag{30}$$

This result can also be derived from (29) by using a standard formula for the WKBJ approximation (e.g. Gill 1980, Eq. (8.12.7)).

Shutts's solution in the spatial domain is the two-dimensional Fourier integral of (30). But this is exactly Maslov's solution (27). To show that the two are equivalent, we first note from (28) that for each normal mode $\zeta = \widehat{\omega}(\mathbf{k}, 0)/\widehat{\omega}(\mathbf{k}, z)$, so that in the hydrostatic approximation $\zeta = m(\mathbf{k}, z)/m(\mathbf{k}, 0)$. It can also be shown that the z-derivative of the phase function $-\mu \log \zeta$ in (30) is equal to m. Thus (30) can be rewritten as

$$\widetilde{\eta} = \widetilde{h}(\mathbf{k}) \left[\frac{m(\mathbf{k}, z)}{m(\mathbf{k}, 0)}\right]^{1/2} \mathrm{e}^{\mathrm{i}\int_0^z m(\mathbf{k}, z')\, \mathrm{d}z'}, \tag{31}$$

which is the quantity in Maslov's Fourier integral (27).

Maslov's method is thus a simplification of the standard transform method involving normal modes. Instead of solving for the normal modes exactly, Maslov's method uses their ray approximation. The exact normal modes cannot generally be determined in a useful analytical form, but the ray approximation is a simple expression that is easily calculated.

The accuracy of Maslov's solution (27) thus depends on how well the ray approximation represents the normal modes. The normal modes are z-dependent, so we expect the ray approximation to be valid when the vertical wave number is slowly varying, i.e. when $|m^{-2}\partial m/\partial z| \ll 1$ (see Lighthill 1978, p. 324).

We rewrite the dispersion relation (2) as

$$m = \frac{KN}{kU + lV} = \frac{N}{U \cos \phi + V \sin \phi}. \tag{32}$$

We allow U and V to be general functions of z, but keep N constant (following Shutts (1998) and as in our comparison below with Shutts and Gadian (1999)). We then obtain

$$\frac{1}{m^2}\frac{\partial m}{\partial z} = -\frac{U_z \cos \phi + V_z \sin \phi}{N}. \tag{33}$$

Hence the ray approximation to the normal modes, and consequently Maslov's method, is accurate for our model when the Richardson number $N^2/(U_z^2 + V_z^2)$ is large.

The condition $|m^{-2}\partial m/\partial z| \ll 1$ used here should not be confused with the condition for ray-theory validity in the spatial domain. We do not know the appropriate condition in the spatial domain, but it cannot be $|m^{-2}\partial m/\partial z| \ll 1$. This is obvious from the discussion in section 2 and from the stationary-phase calculation of Shutts (1998); ray theory breaks down in the region over the mountain even if the Richardson number is large (or infinite, as in the case of Smith 1980). Over the mountain, there are strong gradients in the horizontal wave numbers, which violate the slowly varying assumption. These strong gradients are irrelevant when seeking a ray approximation to the normal-mode equation because the horizontal wave numbers are then treated as constants.

(Note that in the derivation of (33) from (32), ϕ was not differentiated with respect to z because k and l, and hence ϕ, are fixed for each mode. For the spatial domain, k and l are considered to be functions of all spatial coordinates. But, as discussed in section 2, each vertical plane contains waves of the same ϕ, so $\phi_z = 0$. Thus the expression given in (33) is correct for the spatial domain as well. It is the validity condition $|m^{-2}\partial m/\partial z| \ll 1$ that is not appropriate for the spatial domain.)

In deriving Maslov's solution (26), we did not make the hydrostatic approximation. There is a complication, however, in applying Maslov's theory to non-hydrostatic waves. The ray approximation to the normal mode diverges at a buoyancy-frequency turning point where c_{g3} vanishes. The divergence is evident from the constancy of $c_{g3}\tilde{A}(\mathbf{k}, z)$ in (20) and represents a caustic in the wave-number domain. One possible remedy is to use an Airy-function approximation to the normal mode near its caustic, though we have not tried this, nor have we yet considered trapped modes.

We can add rotation to the Maslov solution, but again there are complications. In the rotating case, another factor is introduced into the relation between vertical displacement and wave-action density in (13) (see Eq. (34) of Broutman *et al.* (2001)). This factor carries through the subsequent analysis and appears in the integrand of (26) as another ratio between values at $z = 0$ and at z. The first complication (e.g. Inverarity and Shutts 2000, p. 2712) is that in the general rotating case the mean density has horizontal variations imposed by the thermal-wind relation. Thus the horizontal wave numbers k, l are not constant along the ray, though such variations in k, l may be unimportant in some cases of interest. A second possible complication is that the standard ray approximation to the normal-mode equation fails to satisfy the slowly varying assumption near a rotating critical layer (Yamanaka and Tanaka 1984). A third complication is the presence of an infinitely long lee-wave train of near-inertial oscillations (Shutts 2001). This causes errors due to periodic wrap-around effects when the Fourier integral in Maslov's solution is approximated by a discrete transform (as in the upcoming example). The use of a complex frequency to damp the inertia oscillations and limit their horizontal extent is discussed in Shutts (2001).

In the following we continue to restrict attention to the hydrostatic case without rotation.

4. An example from Shutts and Gadian (1999)

We compare Maslov's method with the numerical results shown in Fig. 11 of Shutts and Gadian (1999). Although they use a nonlinear non-hydrostatic model, their choice of parameters favours a linear hydrostatic response. For this case, the response compares well with the linear hydrostatic theory also developed by Shutts and Gadian. Normal modes are used in the theory but, since these have a very complicated analytical form,

Shutts and Gadian found it simpler to integrate the normal-mode equation numerically, in its exact form. As we have discussed in the previous section, Maslov's method uses a ray approximation to the normal modes.

Shutts and Gadian (1999) have, in fact, supplied a test of Maslov's method. One of their numerical simulations is compared against the theory of Shutts (1998) who, as we mentioned in section 3(c), derived a special case of Maslov's solution. The agreement between the numerics and Shutts's theory is very good in this case, as indicated by Figs. 8(d) and 9 of Shutts and Gadian.

For the case in Fig. 11 of Shutts and Gadian (1999), the wind profile is given by

$$\mathbf{U}(z) = U_0[\cos(\pi z/H),\ \sin(\pi z/H)], \tag{34}$$

where $U_0 = 10\ \mathrm{m\ s^{-1}}$ and $H = 12$ km. The mountain height is

$$h(r) = h_0/(1 + r^2/L^2)^{3/2}, \tag{35}$$

where $r = (x^2 + y^2)^{1/2}$, $L = 20$ km, and $h_0 = 100$ m. In terms of the horizontal-wavenumber magnitude K, the Fourier transform of $h(r)$ is (Smith 1980; Shutts 1998)

$$\widetilde{h}(K) = (2\pi)^{-1} h_0 L^2 \exp(-KL). \tag{36}$$

From (34), the term under the square root in the integrand of Maslov's integral (27) becomes

$$m(\mathbf{k}, z)/m(\mathbf{k}, 0) = k/[k\cos(\pi z/H) + l\sin(\pi z/H)]. \tag{37}$$

The phase function in (27) can be evaluated analytically as

$$\int_0^z m(\mathbf{k}, z')\,\mathrm{d}z' = \frac{2NH}{U\pi}\left[\tanh^{-1}\left(\frac{k\tan(\pi z/2H) - l}{K}\right) + \tanh^{-1}\left(\frac{l}{K}\right)\right]. \tag{38}$$

The mean-density profile in Shutts and Gadian corresponds to $N = 0.0113\ \mathrm{s^{-1}}$, and the Richardson number $N^2/|\mathbf{U}_z|^2$ is approximately 19. To account for the growth in wave amplitude due to the decrease in mean density with height, the dependent variables calculated below are multiplied by $\exp(z/2H_\rho)$ (see section 6.14 of Gill (1982)). We use a density scale height of $H_\rho = 7.5$ km, consistent with typical values for the troposphere (Gill 1982, p. 50).

The Maslov solutions for the x and z perturbation velocities, u and w, respectively, are needed in order to compare with Shutts and Gadian's results. The conversion from vertical displacement η in (27) to u and w is accomplished by ray approximation. For gravity waves, the required ray relations are $\widetilde{w} = -\mathrm{i}\widehat{\omega}\widetilde{\eta}$ and $\widetilde{u} = -km\widetilde{w}/K^2$. The Maslov expression for w, for example, is (27) with the integrand multiplied by $-\mathrm{i}\widehat{\omega}$.

Maslov's Fourier integral is approximated using a discrete Fourier transform, with $\pm k$ wave numbers included as complex conjugate solutions (Smith 1980). In the example below we used a 256 by 256 grid of k, l wave numbers (including complex conjugates), with maximum wave-number magnitudes of $k_{\max} = 8/L$ and $l_{\max} = 6/L$, L being the mountain width. Doubling $k_{\max}$ and $l_{\max}$ (with the same total of 256^2 wave numbers) led to very similar results, except for some noticeable periodic wrap-around effects in the case of Fig. 3(c). Halving $k_{\max}$ and $l_{\max}$ led to significant short-scale errors, especially in the cases of Figs. 3(c) and (d), where peak values decreased by about 30%.

In Fig. 3, we plot the Maslov solutions for u (panels (a) and (c)) and w (panels (b) and (d)) that correspond to Fig. 11 of Shutts and Gadian. These are given at $z = 2.1$ km (panels (a) and (b)) and at $z = 6.3$ km (panels (c) and (d)). For the k, l grid we have

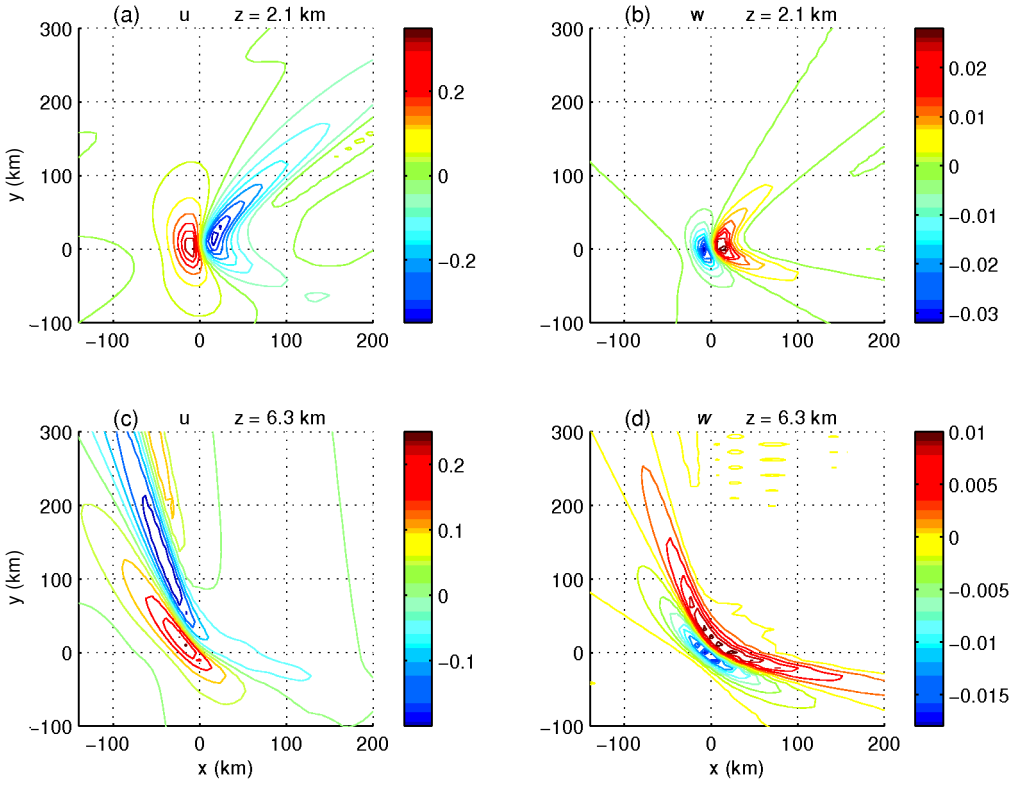

Figure 3. The Maslov solution for the case in Fig. 11 of Shutts and Gadian (1999). The plots show the perturbation velocities u and w at the heights indicated above each panel. The contour interval (CI) and the minimum and maximum values of the variables are (a) CI = 0.05, (−0.38, 0.35), (b) CI = 0.004, (−0.035, 0.030), (c) CI = 0.05, (−0.25, 0.26), (d) CI = 0.002 (−0.018, 0.012).

chosen, the full domain is about 2011 km by 2680 km. Beyond these distances the solution wraps around periodically.

The Maslov solutions are in reasonable agreement with Shutts and Gadian (1999). For example, for the w solution in Fig. 3(b), the Shutts and Gadian contours show a minimum value somewhere between −0.028 and −0.032 and a maximum value somewhere between 0.028 and 0.032. The corresponding minimum and maximum Maslov values are approximately −0.035 and 0.030. The ranges for the other Maslov solutions are given in the caption.

5. Discussion

When the slowly varying approximation breaks down in the spatial domain, the idea of Maslov's method is to look instead to the wave-number domain for a slowly varying ray solution. A spatial solution is then obtained by inverse Fourier transform, giving Maslov's result (27). Away from the caustic over the mountain, the inverse Fourier transform takes on its stationary-phase asymptotic limit and thus duplicates the standard spatial ray solution in which one ray makes the dominant contribution at each position. Near the caustic over the mountain, a spectrum of rays contributes significantly to the wave field at each position, and this too is automatically represented by the inverse Fourier transform. In other applications, other types of caustics occur, each properly

represented in Maslov's method by the inverse Fourier transform in the appropriate asymptotic limit.

Several features of our model have made the implementation Maslov's method very straightforward. At the end of section 3 we noted the potential difficulties that we avoided by our assumption of hydrostatic waves (which eliminates turning points and trapped modes) and from our neglect of rotation. We also emphasize that many applications, unlike the present one, will lead to caustics in both the wave-number and spatial domains. Maslov's method must then combine ray solutions from both domains. Brown (2000) demonstrates how this can be done in a model of surface gravity waves.

The present work represents another step in our development of ray-tracing schemes for internal gravity waves. A previous study concerned the (spatial-domain) initialization of the ray-tracing, and was discussed by Broutman *et al.* (2001). This initialization is suitable for a number of sufficiently idealized models involving radiation from a localized source, including those models that describe internal gravity waves generated by flow over topography, by a collapsing mixed region (Bühler *et al.* 1999; Bühler and McIntyre 1999), and possibly by buoyancy oscillations in clouds (e.g. Piani *et al.* 2000). An important need now is a practical way to correct the spurious amplification associated with the approach to a caustic, or the near miss of a caustic. Our initial experience with Maslov's method here shows that it can be helpful in this regard. Further work, especially with non-hydrostatic and rotation effects included, is required to understand the potential of Maslov's method and the range of applications for which it can bring useful insights.

ACKNOWLEDGEMENTS

We thank the reviewers and Glenn Shutts for their comments. This research was partially supported by the National Aeronautics and Space Administration (NASA) Office of Earth Science's Atmospheric Chemistry Modeling and Analysis Program (grants L68786D and W19946) and NASA Office of Space Science's Geospace Sciences Program (grant W19862). Additional funding was provided by the Office of Naval Research through the Turbulence and Wakes Program (Dr L. Patrick Purtell, program manager) under contract number N00014-99-C-0270.

REFERENCES

Berry, M. V. 1981 'Singularities in waves and rays'. Pp. 455–543 in Les Houches, Session XXXV, 1980, North Holland, Ed. R. Balian

Broad, A. S. 1999 Do orographic gravity waves break in flows with uniform wind direction turning with height? *Q. J. R. Meteorol. Soc.*, **125,** 1695–1714

Broutman, D., Rottman, J. W. and Eckermann, S. D. 2001 A hybrid method for wave propagation from a localized source, with application to mountain waves. *Q. J. R. Meteorol. Soc.*, **127,** 129–146

Brown, M. G. 2000 The Maslov integral representation of slowly varying dispersive wavetrains in inhomogeneous moving media. *Wave Motion*, **32,** 247–266

Bühler, O. and McIntyre, M. E. 1999 On shear-generated gravity waves that reach the mesosphere. Part II: Wave propagation. *J. Atmos. Sci.*, **56,** 3764–3773

Bühler, O., McIntyre, M. E. and Scinocca, J. F. 1999 On shear-generated gravity waves that reach the mesosphere. Part I: Wave generation. *J. Atmos. Sci.*, **56,** 3749–3763

Gill, A. E. 1982 *Atmosphere-ocean dynamics*. Academic Press

Inverarity, G. W. and Shutts, G. J. 2000 A general linearized vertical structure equation for the vertical velocity: Properties, scalings and special cases. *Q. J. R. Meteorol. Soc.*, **126,** 2709–2724

Kravtsov, Y. A. and Orlov, Y. I. 1993 *Caustics, catastrophes, and wave fields*. Springer-Verlag

Lighthill, M. J.	1978	*Waves in fluids*. Cambridge University Press, UK
Maslov, V. P. and Fedoriuk, M. E.	1981	*Semi-classical approximation in quantum mechanics*. D. Reidel
Piani, C., Durran, D., Alexander, M. J. and Holton, J. R.	2000	A numerical study of three-dimensional gravity waves triggered by deep tropical convection and their role in the dynamics of the QBO. *J. Atmos. Sci.*, **57,** 3689–3702
Shutts, G. J.	1998	Stationary gravity-wave structure in flows with directional wind shear. *Q. J. R. Meteorol. Soc.*, **124,** 1421–1442
	2001	A linear model of back-sheared flow over an isolated hill in the presence of rotation. *J. Atmos. Sci.*, **58,** 3293–3311
Shutts, G. J. and Gadian, A.	1999	Numerical simulations of orographic gravity waves in flows which back with height. *Q. J. R. Meteorol. Soc.*, **125,** 2743–2765
Smith, R. B.	1980	Linear theory of stratified hydrostatic flow past an isolated mountain. *Tellus*, **32,** 348–364.
Sonmor, L. J. and Klaassen, G. P.	2000	Mechanisms of gravity wave focusing in the middle atmosphere. *J. Atmos. Sci.*, **57,** 493–510
Thomson, C. J. and Chapman, C. H.	1985	An introduction to Maslov's asymptotic method. *Geophys. J. R. Astronom. Soc.*, **83,** 143–168
Yamanaka, M. D. and Tanaka, H.	1984	Propagation and breakdown of internal inertio-gravity waves near critical levels in the middle atmosphere. *J. Meteorol. Soc. Jpn.*, **62,** 1–17
Ziolkowski, R. W. and Deschamps, G. A.	1984	Asymptotic evaluation of high-frequency fields near a caustic: An introduction to Maslov's method. *Radio Sci.*, **19,** 1001–1025